

Atom Interferometry in Space: Thermal Management and Magnetic Shielding

Alexander Milke,¹ André Kubelka-Lange,¹ Norman Gürlebeck,^{1, a)} Benny Rievers,¹ Sven Herrmann,¹ Thilo Schuldt,² and Claus Braxmaier^{1, 2}

¹⁾ *Center of Applied Space Technology and Microgravity (ZARM), University Bremen, Am Fallturm, 28359 Bremen, Germany*

²⁾ *DLR Institute for Space Systems, Robert-Hooke-Str. 7, 28359 Bremen, Germany*

(Dated: 27 October 2018)

Atom interferometry is an exciting tool to probe fundamental physics. It is considered especially apt to test the universality of free fall by using two different sorts of atoms. The increasing sensitivity required for this kind of experiment sets severe requirements on its environments, instrument control, and systematic effects. This can partially be mitigated by going to space as was proposed, for example, in the Spacetime Explorer and Quantum Equivalence Principle Space Test (STE-QUEST) mission. However, the requirements on the instrument are still very challenging. For example, the specifications of the STE-QUEST mission imply that the Feshbach coils of the atom interferometer are allowed to change their radius only by about 260 nm or $2.6 \cdot 10^{-4} \%$ due to thermal expansion although they consume an average power of 22 W. Also Earth's magnetic field has to be suppressed by a factor of 10^5 . We show in this article that with the right design such thermal and magnetic requirements can indeed be met and that these are not an impediment for the exciting physics possible with atom interferometers in space.

PACS numbers: 03.37.-b, 07.20.-n, 07.55.Nk, 07.87.+v

I. INTRODUCTION

One of the biggest challenges in current theoretical physics is that of finding a valid theory of quantum gravity. Although many theories were proposed, ultimately this question has to be resolved experimentally. Thus, many experiments regarding tests of the fundamental assumptions of gravity and its basic effects were carried out and suggested including tests of the Universality of Free Fall (UFF). This basic principle is a cornerstone of Einstein's theory of gravity and implies that the trajectories of freely falling, structureless test particles in a gravitational field only depend on their initial position and velocity. In particular, the path of such test particles is independent of their composition. A violation of this principle measured by the Eötvös ratio would help to discriminate between the different proposed theories of quantum gravity and it would point in the right direction for further theoretical and experimental development. If the UFF holds to the tested accuracy, bounds will be placed on the viable alternative theories.

A very thriving tool to test the UFF using quantum matter is dual species atom interferometry,¹⁻³ where two atomic clouds propagate freely and their trajectories are compared. Although the advances along this avenue are tremendous, very stringent requirements have to be satisfied to reach down to an accuracy of the UFF test comparable to the classical tests like lunar laser ranging⁴ and torsion balance experiments.⁵ In the present paper, we show that the requirements regarding the magnetic field

and the thermal requirements, which are closely tied to each other, can indeed be satisfied. As a source for specific requirements we refer to the Spacetime Explorer and Quantum Equivalence Principle Space Test (STE-QUEST) mission, which is a medium-size candidate mission in the Cosmic Vision Program of the European Space Agency. Different aspects of the STE-QUEST mission are described in Ref. 6-9. The specific requirements for STE-QUEST are derived in Ref. 10.

The STE-QUEST atom interferometer was designed with heritage from projects such as the DLR project QUANTUS¹¹ (QUANTengase Unter Schwereelosigkeit) and the CNES project I.C.E.¹² (Interférométrie Cohérente pour l'Espace). In QUANTUS, experiments with Rubidium (Rb) Bose-Einstein condensates are carried out in the drop tower at ZARM in Bremen and are currently prepared for a sounding rocket by the end of 2014.¹³ A dual species interferometer is already included in I.C.E., where the experiment is performed in parabolic zero-g flight.

The experimental sequence foreseen for STE-QUEST, is to cool two ensembles of ⁸⁵Rb and ⁸⁷Rb atoms down to Bose-Einstein condensation in two steps. First atoms are loaded from a magneto-optical trap into a magnetic trap on an atom chip for evaporative pre-cooling. Then, they are loaded into an optical dipole trap for final evaporative cooling. During this step a strong homogeneous magnetic field of 160 G is applied in order to tune atomic interactions using a so called Feshbach resonance. The magnetic field is generated by two coils in Helmholtz configuration with a middle distance of 105 mm, a coil's mean diameter of 206 mm, and equal electrical current of 4.8 A flowing in the same direction. This way, two Bose-Einstein condensates of 10^6 atoms shall be generated and released from

^{a)} Electronic mail: norman.guerlebeck@zarm.uni-bremen.de

the trap to fall freely in Earth's gravitational field. A detailed description of the atom interferometer design of STE-QUEST can be found in Ref. 9.

The article is organized as follows: In Sec. II, the thermal requirements and the requirements for the magnetic shielding are summarized for the example of the STE-QUEST atom interferometer. Subsequently, the methods and models used for the analysis of the thermal control system and the magnetic shielding are discussed in detail. The results are summarized in Sec. IV.

II. THERMAL AND MAGNETIC SHIELDING REQUIREMENTS

The sensitivity of a test of the UFF using dual species atom interferometry depends on how well spurious differential accelerations can be suppressed below the shot noise level of $2.9 \cdot 10^{-12} \text{ m/s}^2$ ¹⁰. In STE-QUEST, one such differential acceleration signal comes from the fact that both atom species couple differently to a magnetic field via the linear and quadratic Zeeman effect. During the interferometer sequence a homogeneous magnetic quantization field of $B_0 = 100 \text{ nT}$ is applied and spatial variations of this field over the interferometer baseline of 12 cm have to be kept below 1 nT^{10} . Additionally, an even stronger requirement of $\delta B/dz < 0.3 \text{ nT/m}$ has to be met during the preparation of the Bose-Einstein condensates, where a strong homogeneous Feshbach field is required. The source of such magnetic field variations can be an external one like Earth's magnetic field. As a consequence, the experiment has to be shielded against its influence. On the other hand, magnetic field fluctuations and gradients produced by the instrument itself during the preparation of the Bose-Einstein condensates appear inside the magnetic shielding. These depend on the precise geometry, which can be affected by thermal expansion, and an elaborate thermal control system has to be designed and verified to keep these systematic effects below the required levels¹⁰. We discuss both issues, the thermal control as well as the magnetic shielding, subsequently.

A. Thermal Control System

The most critical issues for the sensitivity of an atom interferometer originating from thermal effects are temporal and spatial fluctuations of the magnetic fields, which are used to manipulate the atomic ensemble. These fluctuations are mainly caused by changes in position and length of the magnetic coils, in particular, the Feshbach coils resulting from thermal expansion. The thermal stability requirements have to be guaranteed during the entire measurement cycle. To reach the aforementioned requirement for the magnetic field gradient of $\delta B/dz < 0.3 \text{ nT/m}$, the Feshbach coils have to be designed such that they are very close to Helmholtz con-

figuration. To achieve this, a numerical simulation based on the Biot-Savart law was performed with 400 windings for each coil. The packing of the windings is essential in these simulations. Starting from an optimal position of distance and coil diameter for all windings found numerically, the effects of thermal expansion are tested along the z-axis in an area with a diameter of $40 \mu\text{m}$ placed symmetrically between the coils. The BEC will be located in that region during preparation, when the Feshbach coils are used. The temperature stability requirement is calculated due to maximum allowed position change from the ideal Helmholtz configuration of the coil's middle distance (105 mm) and middle diameter (206 mm) by linear thermal expansion of the copper windings, Torlon mounting pads, aluminum holdings and the titanium vacuum chamber (see Tab.I).

Component		Requirement
FC	Diameter change	$\Delta d < 520 \text{ nm}$
FC	Distance change	$\Delta l < 320 \text{ nm}$
FC	Temp. stability	$\Delta T < 0.15 \text{ K}$
VC	Temp. stability	$\Delta T < 0.30 \text{ K}$

TABLE I. Requirements on the TCS for Feshbach coils (FC) and vacuum chamber (VC) on which the Feshbach coils are mounted.

B. Magnetic Shielding

Fluctuating external magnetic fields can be a major source of systematic errors in atom interferometry measurements. Also, small spatial inhomogeneities and gradients of the magnetic field can lead to significant systematic phase shifts as explained in the beginning of Sec. II. Thus, a high performance magnetic shielding is required for the targeted performance of atom interferometers including the dual atom interferometer foreseen in STE-QUEST.

The temporal fluctuations of external magnetic fields are mainly due to the satellite's movement through Earth's magnetic field, $B_{Earth} \approx 50 \mu\text{T}$. These fluctuations need to be shielded by at least a factor of $S > 10000$, i.e. to the low nT level. This shielding effectiveness factor $S_{x,y,z}$ is defined by

$$S_{x,y,z} = \frac{B_{x,y,z}^{outside}}{B_{x,y,z}^{inside}} \quad (1)$$

with $B_{x,y,z}^{outside}$ as the outer magnetic field and $B_{x,y,z}^{inside}$ as the residual inner magnetic field inside the shielding.¹⁴

Even more critical than the shielding of temporal fluctuations is the requirement on the spatial gradients of the magnetic field along the interferometer baseline of $L = 12.4 \text{ cm}$. Two systematic effects need to be considered here: a small differential acceleration of the two

clouds after preparation due to the linear Zeeman effect and the quadratic Zeeman shift during the interferometer sequence. While mitigation strategies to alleviate both effects have been identified in STE-QUEST,¹⁰ the requirement on the magnetic field gradients to be met still remains challenging and no gradient larger than 1 nT/12 cm is allowed (larger than 1 nT over the baseline L).

The high shielding factor is reached by using a μ -metal enclosure. This magnetically soft nickel-iron alloy has a high permeability μ_r from 30000 to 50000, which results in a good shielding performance. Shield designs with multi-layered μ -metal shells can further improve the performance of the shielding.¹⁴ In addition to a passive shielding with μ -metal, an active compensation by coils can improve the homogeneity and stability of the magnetic fields inside the experiment.¹⁵

III. METHODS AND MODELING

A. Thermal Management

The thermal management of an atom interferometer in space is challenging, since the environmental condition may change rapidly due to orbital shadowing followed by direct sunlight. Furthermore, convective heat transfer is negligible and heat exchange within the system and with the environment has to be managed only by radiation and conduction. In order to ensure the functionality of the atom interferometer and its thermal control system (TCS) over the entire mission period, the TCS has to be tested extensively in advance.

Further difficulties arise from the fact that the instrument itself produces high amounts of waste heat. For example, the electronics and in particular the magnetic coils are considerable sources of heat within the instrument. Thus, the TCS has to be adjusted such that this heat is transported to the satellite's heat sink in accordance with the requirements summarized in Sec. II A. A major challenge for this is the cyclical instrument operation resulting in a fluctuation of the magnitude of the heat fluxes. To ensure robustness and to avoid disturbances on the instruments by pumps, which would yield artificial accelerations beyond the acceptable level,¹⁰ the TCS has to be designed as a completely passive subsystem.

In order to develop a design for the atom interferometer's TCS, which fulfills the requirements listed in Tab. I, a 3D finite-element model (FE) of the atom interferometer physics package has been set up in ANSYS classic.¹⁶ This model is used for the definition of the thermal interfaces between physics package and bus, for testing and validation of the thermal stability of the design within operational requirements as well as for a general optimization of the design with respect to perturbative influence of thermal effects on the atom interferometer performance. The general approach for the design of the TCS

as well as details on the thermal aspects of the instrument will be discussed in Secs. III A 1-2.

1. General Approach

The main task of the TCS of the atom interferometer is to assure a stable operation of the instruments within the specified temperature requirements. Furthermore, the waste heat generated by the instruments has to be transported to the satellite bus heat sink and the influence of changing environmental conditions has to be buffered out.

In order to realize this, different options for thermal heat transport are available. For the design of the TCS we considered the buffering of thermal perturbations by means of phase change materials (PCM) as well as the transport of heat by means of heat pipes and thermal straps. While PCM realizes a general low perturbation level leading to a largely uniform temperature distribution, the changing mass distribution during phase change introduces spurious accelerations of the Bose-Einstein condensates due to changing gravity gradients. A mitigation strategy for this would be possible by applying a filler matrix. However, the complexity of the involved hardware would be considerably increased. The use of heat pipes would provide a very efficient way to realize high heat flows between instruments and heat sink. But it has to be considered that heat pipes show a start-up phase and are working less efficient in direction to the gravitational field. In addition to this, they show self-gravity effects similar to PCM arising from the phase change of the contained fluid during heat transport. Apart from this, the layout of a heat pipe system, in particular the required diameters for the capillary and heat pipe circle, would be challenging with respect to the requirements for magnetic shielding of the atom interferometer. With these arguments in mind, heat strap connections can be identified as the best option for thermal transport within the atom interferometer and to the satellite bus. They transfer a considerable amount of heat while offering flexible layout and dimensions within the specified design requirements. Comparing to copper ($\lambda = 360 - 400$ W/Km) and nickel silver ($\lambda = 26 - 40$ W/Km), the carbon fibers show a much higher thermal conductivity ($\lambda = 800$ W/Km). Additionally the mass is reduced due to the very low density of those fibers¹⁷.

A suitable design is shown in Fig. 1. Because of the position in the bus and to avoid thermal couplings, the atom interferometer is divided into four subsystems: the physics package, the Extended Cavity Diode Laser (ECDL) and Master Oscillator Power Amplifier (MOPA), the laser periphery and the electronic box. These subsystems are temperature stabilized by means of three cold plates. The physics package's cold plate is thermally connected with the middle plate, which is the heat sink of the satellite, by a high conductive car-

bon fiber heat strap through the μ -metal. The middle plate is temperature stabilized to $(13 \pm 3)^\circ\text{C}$ by the TCS of the satellite bus. The laser system and the electronic box cold plates are mounted directly on the middle plate. Due to the very strict temperature requirements of the ECDL and MOPA, they have to be cooled actively by thermo-electric coolers.

The temperature stabilization of the laser system and the electronic box is a well elaborated technique, which is realized in many laboratories worldwide and will not be discussed here. The main focus is the thermal management of the physics package and its instruments, which will be presented in Sec. III A 2.

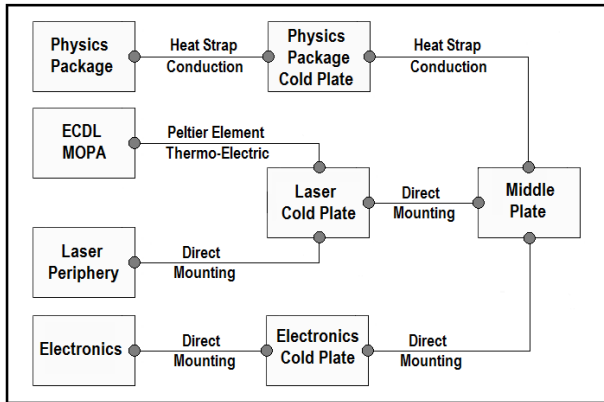


FIG. 1. General thermal control system approach for the atom interferometer.

2. Physics Package

The TCS of the physics package is challenging especially concerning the magnetic coils positioned inside the μ -metal shield. On the one hand, the acceptable thermal gradient over the coils is limited, since any thermal expansion affects the magnetic field and, thus, the atom interferometer performance. Therefore, any heat produced by the coil operation has to be transported quickly out of the system. The coils produce a large amount of heat demanding a high heat transport rate, which can be realized by increasing the size of the thermal interfaces. On the other hand, a large diameter of the feed-throughs decreases the shielding effectiveness factor S of the μ -metal. Hence, the maximum size of the heat strap connecting the physics package and the middle plate is limited. Nevertheless, the discussion in Sec. IV B 1 points out that a feed-through diameter size of 40 mm for a thermal connection is acceptable with respect to magnetic shielding in our design and keeps thermal deformation within the acceptable range. Furthermore, the main heat sources are not operating constantly, but periodically at specific times during a 20s measurement cycle. The main heat sources included in the model and their individual opera-

tion time are listed in Tab. II. This time-varying schedule is especially demanding concerning the temperature stability requirement of the instruments and the mitigation of the deformation of the Feshbach coils by thermal expansion. In order to keep the temperatures of the physics package components stable, a set of high conductive carbon fiber heat straps with individually designed diameter sizes are applied for heat transport. Each of them is thermally connected to the physics package cold plate, which is a temperature stabilized heat storage, heat exchange and thermal interface mounting unit.

Due to a limited influence on the overall heat budget, thermal radiation from the instrument to the magnetic shield and thermal conduction through the holding structure is neglected in this model allowing for a higher computational performance. Since these additional minor heat transport mechanisms would only increase the overall heat exchange and homogenize the system thermally, they would even improve the performance of the TCS. In this sense, the model implements a thermal worst case scenario.

Component	Operation Time [s]	Peak Power [W]	Averaged Power [W]
Meso U	0-2	22.5	2.25
2DMOT	0-2	13	1.3
Offset 1	0-2	2x32.5	2x3.25
Meso H	2-2.1	50	0.25
Base-chip	2-2.1	50	0.25
Science-chip	2-5.6	8	1.44
FCs	5.6-8.9	2x67.5	2x11.1375
CCD Camera	10-20	5	2.5
Dispenser Heater	0-20	constant 40 °C	constant on 40 °C

TABLE II. Measurement cycle of 20s of the atom interferometer and heat loads generated by the instrument's subsystems, which are included in the FE-model.

The thermal design of the physics package is shown in Fig. 2. In this design, only the main heat sources and high mass components, which are dominant for the overall heat budget are considered. The thermal connections are shown schematically as heat strap connection (thick line), mounting connection (triangle line) and thermal insulation (crossed out line). One of the critical parts of the physics package is the vacuum chamber with attached telescopes for interferometry, cooling, and detection. As mentioned in Sec. II A, a thermal expansion of the vacuum chamber has to be minimized. In order to satisfy this requirement, the vacuum chamber is thermally isolated by Torlon pads¹⁸ to the Feshbach coils as well as to the CCD camera telescope. The highly conductive carbon fiber heat straps are connecting the main heat sources to the physics package cold plate. The diameter of each heat strap has been individually calculated. The heat transport through the mounts and screws between

the different components is considered here by means of idealized FE models as well to assess the thermal properties of the individual mechanic interfaces.

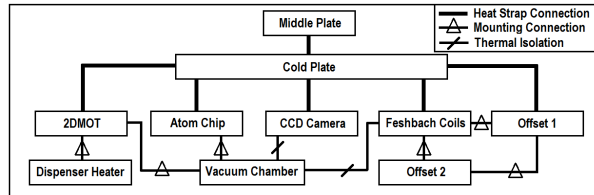


FIG. 2. Thermal control system design of the physics package.

Based on this design and the geometries of the atom interferometer physics package, a FE-model has been created (see Fig. 3 top). This FE-model is an idealization of the physics package geometry design. The complex geometrical structure of the telescopes have been idealized by representative bodies implementing equivalent geometric diameters and component masses as defined by the STE-QUEST study design.⁹ Furthermore, we take the influence of the wire isolation material and the gaps between the wires into account by assuming that the magnetic coils (light blue) are made of copper with reduced conductivity ($\lambda = 80 \text{ W/mK}$) and reduced density ($\rho = 5800 \text{ kg/m}^3$). The dispenser heaters are assumed to be of porous titanium with a reduced conductivity ($\lambda = 1.5 \text{ W/mK}$) and a reduced density ($\rho = 1526 \text{ kg/m}^3$). The vacuum chamber is made of titanium (green) and the coil holders are made of aluminum (red). The coil holders are used for mounting the heat straps and as a thermal interface of the coils. The heat straps (ultramarine) are of highly conductive ($\lambda = 800 \text{ W/mK}$)¹⁷ and flexible carbon fibers as well as the connection to the middle plate. The cold plate (pink) is of highly conductive copper ($\lambda = 390 \text{ W/mK}$). The atom chip, which is inside the vacuum chamber is connected with the TCS via a copper gasket on the vacuum chamber. The insulation between the Feshbach coils and the vacuum chamber is realized by Torlon pads. The charge-coupled device (CCD) camera is mounted inside an aluminum box on top of the telescope, which is thermally isolated by a layer of Torlon (dark blue). The middle plate is temperature stabilized to $(13 \pm 3)^\circ\text{C}$ by the TCS of the satellite bus. The mounting connections between the components are represented by direct node-to-node 3D-LINK elements (blue lines). The whole system has to be thermalized from a uniform temperature of 13°C first to reach equilibrium temperatures of the components and to achieve the necessary temperature gradients for the heat fluxes. By means of an optimization of the thermal performance of this FE-model the required individual heat strap's diameter size is calculated and included in the computer aided design (CAD) model (see Fig. 3 bottom).

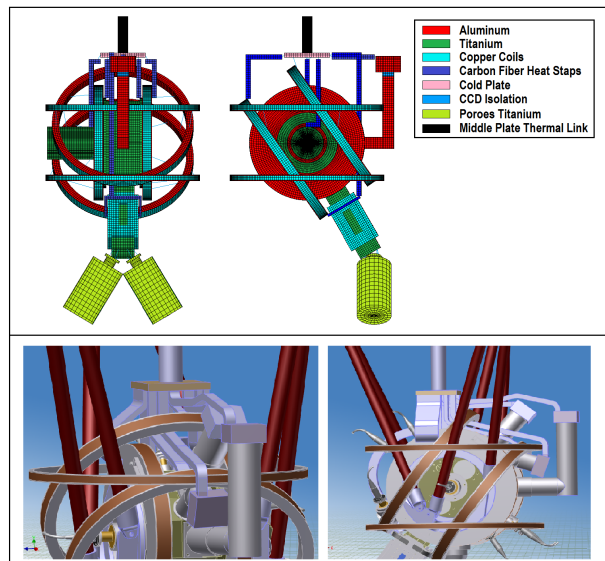


FIG. 3. **Top**: Meshed FE-model of the atom interferometer physics package. **Bottom**: CAD-model of the atom interferometer physics package with the thermal interfaces.

B. Magnetic Shielding

Based on previous FE simulations for the MAIUS and PRIMUS projects^{13,19} a shielding design with four individual layers of μ -metal was designed in CAD. In this model, each layer has a thickness of 1 mm and consists of two parts, a cylindrical shell with welded bottom plate and a cover with welded overlap (as shown in Fig. 4). The best shielding factor was achieved in simulation for gaps between the μ -metal layers of 13 mm in radial and 35 mm in axial direction while at the same time keeping the net mass of the magnetic shield as small as possible. This shielding design provides several feed-throughs for the TCS and supplies of the atom interferometer. An opening for a vacuum tube (25 mm diameter), which connects the pump section with the vacuum chamber inside the magnetic shield, is foreseen on the top of the shielding. Next to this feed-through, we consider an opening (40 mm diameter) for the heat straps, which connect the experiment to the middle plate, cf. Sec. II A. Six more feed-throughs (33 mm diameter) are implemented in the design on the top of the shields to account for the mounting structure, which connects the instrument to the middle plate. All openings are drilled through all four layers. On the side of the cylindrical μ -metal layers, a rectangular feed-through ($100 \times 55 \text{ mm}^2$) is implemented for electrical cables and optical fibers. The rectangular openings are rotated by 90° to each other to compensate magnetic leakage through the opening inside the shielding. Additionally, an opening for a demagnetization cable is provided on the side in the lower region of the cylindrical layers. The overall mass of the complete shielding including mounting material is approximately

53 kg.

The shielding properties of this design were analyzed by means of FE simulation, too. To simulate the effect of the Earth's magnetic field, the CAD model of the shielding was placed inside a virtual enveloping body, which generated a magnetic field of $B = 40 \mu\text{T}$. The residual magnetic field inside the magnetic shielding is evaluated within virtual small test bodies at the position of the atom interferometer in the middle of the shielding. The permeability of the μ -metal was set to $\mu_r = 30000$ (manufacturer information²⁰).

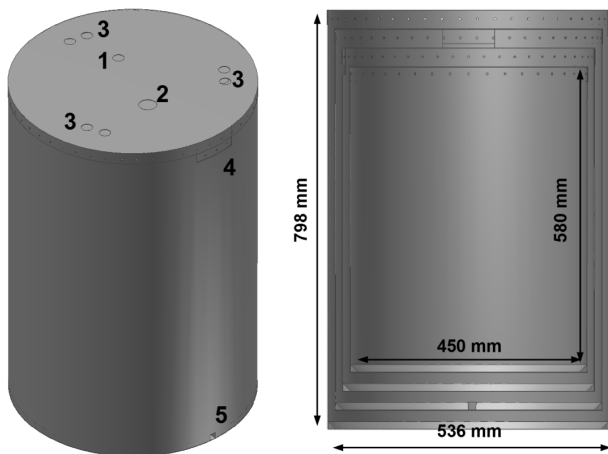


FIG. 4. **Left:** View of the complete magnetic shielding with visible feed-through openings: 1) vacuum pipe, 2) heat strap, 3) mounting rack, 4) cables and fibers, 5) degaussing coil. **Right:** Cross-section of the complete 4-layer magnetic shielding (necessary spacers not shown).

IV. RESULTS

A. Thermal Control System

In order to test the TCS on changing environmental conditions, a variation of the middle plate's temperature of $(\pm 3)^\circ\text{C}$ within two measurement cycles is considered. The temperature evolution of some critical components is shown in Fig. 5. While the atom chip shows periodical variations in the range of 2.5 K directly resulting from the chip operation, the most critical parts like the Feshbach coils and the vacuum chamber show a rather stable temperature evolution. The varying thermal conditions on the atom chip are demanding, since thermal expansions arising from thermal gradients also lead to deformations of the magnetic containment fields. While the in-plane expansion is uncritical considering the isotropy and the low thermal expansion coefficient of the chip substrate, the expansion of the copper mount below the chip may lead to a change of the chip position during the measurement cycle. This effect can be mitigated by a scaling of the chip currents but demands a thorough modeling and

testing with respect to the measurement cycle and the resulting thermal gradients.

Although the environmental temperature changes have an impact on the cold plate's temperature, this effect is rather small on the other components. In addition to the operational case $(13 \pm 3)^\circ\text{C}$, a cold case $(10 \pm 3)^\circ\text{C}$ and a hot case $(16 \pm 3)^\circ\text{C}$ scenario is tested and the results are listed in terms of thermal requirements in Tab. III. The temperature shift in the cold or hot case has no effect on the thermal stability requirements. In summary, it can be stated that the TCS design presented and tested by a FE-model is able to fulfill the thermal requirements, which are set in Tab. I.

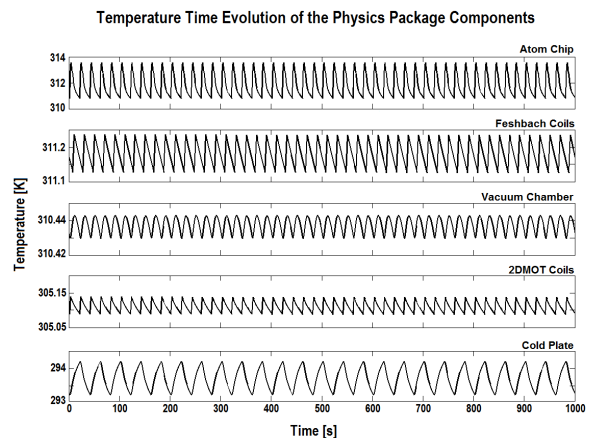


FIG. 5. Volume temperature time evolution of some critical components with alternating environmental conditions $(\pm 3)^\circ\text{C}$.

ΔT_{VC} in K	ΔT_{FC1} in K	ΔT_{FC2} in K
0.014 ± 0.004	0.11 ± 0.03	0.11 ± 0.03

TABLE III. The maximal temperature variations of the vacuum chamber (ΔT_{VC}) and the two Feshbach coils (ΔT_{FC1} and ΔT_{FC2}) for a simulation time of 2000s is shown. The result is the same for the operational, hot and cold case.

B. Magnetic Shielding

1. Shielding effectiveness factor

The results of the FE analysis for the shielding effectiveness factors of the discussed shielding design are summarized in Tab. IV. It should be noted that in FE simulations of magnetic shieldings the modeled shielding effectiveness factor is often better than in reality. This is caused by multiple reasons such as variation within production tolerances, small gaps between components or

mechanical deformation of the assembled shielding. All of this cannot be modeled accurately but strongly affect the actual shielding effectiveness factor. We have, therefore, performed measurements on a prototype magnetic shield of the above design but with three layers instead of four and have shown an actual shielding effectiveness factor that is smaller by a factor of four compared to the FE-modeling results. In order to account for this discrepancy, the FE results for the STE-QUEST four layer shielding shown in Tab. IV have been corrected by this factor. The corrected numbers still indicate that the shielding effectiveness factor of 10000 along all spatial directions will be achieved.

Component of S	FE result
S_x	35000 ± 1500
S_y	35200 ± 1600
S_z	10700 ± 500

TABLE IV. FE simulated shielding effectiveness factor S for the three spatial directions.

2. Magnetic Field Gradient

FE simulations along the cylindrical axis show that the gradient of the field inside the shielding caused by outer magnetic fields is less than $0.1 \text{ nT}/12 \text{ cm}$ as shown in Fig. 6. This is a factor of 10 below the requirements given above. At this level, it can be assumed that field inhomogeneities inside the magnetic shield will be dominated by residual magnetization of the μ -metal shells and not by residual external fields. It is expected that with demagnetization of the magnetic shielding the effect of this residual magnetization can be minimized to a gradient of less than $1 \text{ nT}/12 \text{ cm}$.

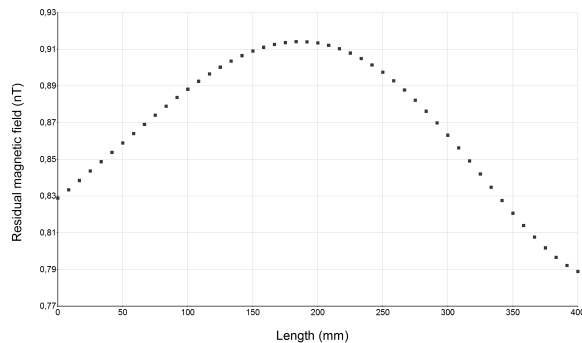


FIG. 6. Results of FE simulation of magnetic field gradients from an external field $B_z^{outside} = 40 \mu\text{T}$ along the cylinder axis. The gradient is $< 0.1 \text{ nT}/12 \text{ cm}$.

V. CONCLUSION

While dual species atom interferometry in space is a powerful and promising tool for fundamental physics science, the technological challenges that have to be overcome in order to realize a sensor offering a high measurement accuracy are considerable. Among these, the thermal management and the magnetic shielding of the sensor hardware have a strong impact on the achievable sensor accuracy. In this paper, we have analyzed the current design of the thermal control system and the magnetic shielding with respect to the STE-QUEST mission specification as a test case scenario. Both systems are designed and verified by means of complex 3D FE models, which have been used to simulate the evolution of heat flows, temperatures and magnetic field gradients for the dynamic boundary condition throughout the STE-QUEST orbit and the measurement cycle. The numeric results show that the current design of the atom interferometer allows to satisfy thermal and magnetic requirements by a thorough design of both the thermal control system and the magnetic shielding. Furthermore a more advanced design of the magnetic coils could help to relax the requirements on thermal expansion. The design and the FE models of both the thermal control system and the magnetic shielding will be used for future optimization or verification of overall design changes arising from other subsystem or mission requirements.

ACKNOWLEDGMENTS

The authors acknowledge inspiring discussions with the members of the STE-QUEST consortium in particular with Johannes Burkhardt and the team at Astrium GmbH in Friedrichshafen. This work was supported by the German space agency (Deutsches Zentrum für Luft- und Raumfahrt – DLR) with funds provided by the Federal Ministry of Economics and Technology under grant numbers 50 OY 1302 and the European Space Agency (ESA).

- ¹A. Peters, K. Y. Chung, and S. Chu, High-precision gravity measurements using atom interferometry, *Metrologia* **38** 25 (2001).
- ²S. Fray et al., Atomic interferometer with amplitude gratings of light and its applications to atom based tests of the equivalence principle, *Phys. Rev. Lett.* **93** 240404 (2004).
- ³A. Bonnin et al., Simultaneous dual-species matter-wave accelerometer, *Phys. Rev. A.* **88** 043615 (2013).
- ⁴J. G. Williams, S. G. Turyshev, and D. H. Boggs, Lunar laser ranging tests of the equivalence principle, *Class. Quant. Grav.* **29**, 184004 (2012).
- ⁵S. Schlamminger et al., Test of the equivalence principle using a rotating torsion balance, *Phys. Rev. Lett.* **100** 041101 (2008).
- ⁶G. Hechenblaikner et al., STE-QUEST mission and system design - Overview after completion of phase-A, *Exp. Astron.*, doi: 10.1007/s10686-014-9373-6 (published online).
- ⁷D. Aguilera et al., STE-QUEST - Test of the Universality of Free Fall Using Cold Atom Interferometry, *Class. Quantum Grav.* **31**, 159502 (3pp), 2014.
- ⁸G. M. Tino et al., Precision gravity tests with atom interferometry in space, *Nucl. Phys. B (Proc. Suppl.)* **243**, 203 (2013).

- ⁹T. Schuldt et al., Design of a space compatible dual species atom interferometer, (unpublished).
- ¹⁰C. Schubert et al., Differential atom interferometry with ^{87}Rb and ^{85}Rb for testing the UFF in STE-QUEST, arXiv:1312.5963v1, 2013.
- ¹¹T. van Zoest et al., Bose-Einstein condensation in microgravity, *Science* **328** 1540 (2010).
- ¹²R.A. Nyman et al.: I.C.E.: a transportable atomic inertial sensor for test in microgravity, *Appl. Phys. B* **84** 673 (2006).
- ¹³See <http://www.iqo.uni-hannover.de/551.html> fo MAIUS - Atom-optical experiments on sounding rockets; accessed 06 January 2014.
- ¹⁴E. A. Burt & C. R. Ekstrom, Optimal three-layer cylindrical magnetic shield sets for scientific applications, *Rev. Sci. Instrum.*, **73** 2699 (2002).
- ¹⁵Ph. Laurent et al., Design of the cold atom PHARAO space clock and initial test results, *Appl. Phys. B* **84** 683 (2006).
- ¹⁶See www.ansys.com for official website of ANSYS, Inc.; accessed 28 December 2013.
- ¹⁷See www.techapps.com for producer of space qualified graphite fiber heat straps; accessed December 2013.
- ¹⁸See www.polytron-gmbh.de/torlon-typen.aspx for data sheet of Torlon 4203 thermal isolation; accessed 28 December 2013.
- ¹⁹See <https://www.zarm.uni-bremen.de/research/space-science/experimental-gravitation-and-quantum-optics/projects/primus.html> for PRIMUS - precision interferometry with matter waves in zero gravity; accessed 18 July 2014.
- ²⁰See <http://www.sekels.com/en/sekels-products/mumetal-mumetall-magnetic-shielding-and-shielding-foils/alloys/> for data sheet of MUMETALL from Sekels GmbH; accessed 06 January 2014.